

APPLIED RESEARCH

From Architecture to Field Trial: A Scheme of mmWave Based IAB and Small Base Station of Commercial Frequency for the Communication of Subway Tunnel Scenario

XIAOYIN ZHAO^{ID}, FEI QI^{ID}, (Member, IEEE), AND WEILIANG XIE^{ID}

Department of Mobile Communication and Terminal Technology, China Telecom Corporation Ltd. Beijing Research Institute, Beijing 102209, China

Corresponding author: Xiaoyin Zhao (zhaoxy5@chinatelecom.cn)

ABSTRACT With the increasing scarcity of spectrum resources and the continuous exploration of high-frequency spectrum resources, millimeter wave (mmWave) has been introduced to 5G deployment scenarios, one of which is the high-speed railway wireless networks. Because of the characteristics of mmWave, it is suitable for Enhanced Mobile Broadband (eMBB) service in subway tunnel scenarios, in which there are increasing data rate requirement of passengers to be satisfied. To this end, we propose a new scheme of Integrated Access and Backhaul (IAB) plus small stations in the carriage, in which the backhaul link is 5G Non-Standalone (NSA) networking with 4G for master node and 5G mmWave for secondary node, so as to overcome the handover burden and penetration loss of mmWave, that is more severe in the high-frequency range. Based on the existing old 4G equipment, mmWave is applied for 5G user-plane connection in NSA dual connection, while the control plane connection still relies on 4G commercial frequency band, in order that even if the millimeter-wave link quality is seriously degraded, the IAB-node can still maintain the connection with the master node and re-establish the mmWave link through the exchange of control information on the 4G low-frequency band. Unlike previous attempts, the proposed approach applies dual link to the backhaul link and 5G commercial frequency band to the in-vehicle access link of small station with Radio Access Network (RAN) sharing technology, so that the bandwidth shared by the operators can be aggregated in one small station and fully used for user access to match the mmWave large bandwidth of the backhaul link. Field trials showed that although the data rates were somewhat unstable at the handover points, which still need to be improved in the future work, the average end-to-end uplink and downlink data rates were greatly improved, compared to the previous average data rates when only outdoor signal penetrating indoors was used in subway tunnel. In addition, the proposed scheme can reduce the operator's construction and maintenance costs by making full use of the existing 4G equipment, which provides a reference for upgrading 4G to 5G signal coverage for all tunnel scenarios.

INDEX TERMS Millimeter wave, 5G, small base station, subway tunnel, high-speed railway, integrated access and Backhaul.

I. INTRODUCTION

The fifth generation (5G) technology is supposed to provide significantly improved performance in the field of data

The associate editor coordinating the review of this manuscript and approving it for publication was Jjun Cheng^{ID}.

rate, reliability, latency, and mobility for different use cases and deployment scenarios. The implementation of the 5G specification has been completed in the Third Generation Partnership Project (3GPP) within the scope of New Radio (NR), with the purpose of developing efficient and flexible designs to fully support different use cases and deployment

scenarios [1]. Railway communications is one of the deployment scenarios, and the evolution of which will be providing fully automated train operation that requires highly reliable communication with moderate latencies at very high speeds of up to 500 km/h [2]. However, before realizing this future vision, we first need to solve the problem of users' demand for larger bandwidth and higher data rates when surfing the internet for eMBB services on the trains running at the speed of 60-120 km/h. Due to the deployments of subways all over the world, to address 5G data surges of subway passengers has gained more and more significant importance. Moreover, many subway tunnels have been previously deployed with 4G base stations, so how to make use of the existing equipment and save equipment investment while allowing subway passengers to experience the performance boosting of the 5G technology is the problem to be solved in this paper.

Tunnel scenario, mostly encountered in subway scenario, is one of the main scenarios of the HST environment. In [3], the HST environment is classified into open space, viaduct, cutting, hilly terrain, tunnels, and stations scenarios. There has been some research work on mmWave channels under the station scenario model in both academia and industry. Simulation of mmWave channels in the subway station scenario model was conducted in [4], and the first 5G smart railway station has been established at Shanghai Hongqiao Railway Station [5]. However, unlike station scenario, tunnel scenario is a special one in all the HST environments, because tunnel propagation can be assumed as an oversize waveguide, which is attributed to that the wavelength of transmission carrier is much smaller than the transversal dimensions of transportation tunnels [6]. Therefore, mmWaves, which is in the high-frequency range with short wavelength and large bandwidth, are suitable for tunnel scenarios. Many studies on the propagation characteristics of radio waves in tunnel scenarios use deterministic or empirical models to predict the fading or latency characteristics of radio wave propagation. However, the prediction model cannot solve all the problems, in particular the penetration loss through the carriage as well as cell handover impacts. In actual tunnels, the attenuation of radio propagation is generally greater than the theoretical prediction value due to factors such as the existing ventilation ducts, railway tracks as well as unevenness of tunnel structure and cell handover for the moving subway carriage. Consequently, the analysis of wireless transmission still requires field trials to get first-hand data, especially for complex subway tunnel environments. In this paper, in order to minimize the penetration loss as well as handover impacts, we design a new scheme of IAB + small stations in the carriage, in which dual connection architecture, cell merge, 5G secondary node, carrier aggregation, and beam forming technologies are applied to backhaul link to obtain stable user control plane connection, smaller handover latency, greater bandwidth, and more concentrated signal energy. Moreover, we also analyze the problems faced by signal transmission in subway tunnel scenarios, with a focus on the characteristics

of mmWaves and their suitability for propagation in tunnels. In the end, a field trial is carried out in the subway tunnel scenario to demonstrate whether there is an increase in user's data rates in the carriage under this approach.

5G millimeter-wave technology has the characteristics of large bandwidth and low latency, which will be an important direction for the next development of 5G. With the use of various multiple access multiplexing technologies, the channel capacity can be greatly improved [7]. It is suitable for high-speed multimedia transmission services, which is undoubtedly very attractive when the frequency resource becomes more and more precious today. On the basis of continuous coverage provided by the Sub-6GHz network, 5G mmWave can be used as a capacity supplement in outdoor or indoor hot spots and other scenarios. The 3GPP Release 15 has introduced mmWave to the 5G Non-Standalone (NSA) networking scenario, primarily for 5G/4G dual connectivity in mmWave spectrum and low or medium frequencies.

NR Integrated Access and Backhaul (IAB) technology, which is called Relay in 4G networks, was originally introduced in 3GPP Release 10 to enable fast and continuous network coverage. Since the continuous coverage of 4G base stations by operators is still acceptable, it has not been widely promoted. However, due to the relatively high frequency band and large penetration loss of 5G network, in view of the limitation of NR coverage in intermediate frequency band and above, IAB technology was introduced again in Release 16 and approved in [8] as technical specification. Moreover, 5G mmWave are currently applied as wireless backhaul networks not only for providing point-to-point fixed services [9], but also for wireless transmission between IAB donor station and IAB-node [10]. As to subway tunnel scenario, an aggregated stream for the backhaul for both inter- and intra- vehicle scenarios need to be transmitted, for which a bandwidth of several GHz is demanded to accommodate high-data rate [11], [12]. These requirements are a powerful driving force for exploring the mmWave band for wireless backhaul link.

Nowadays, millimeter-wave communication for wireless backhaul has aroused widespread interest in academia and industry. Some research has focused on mmWave communications, with both industry and research groups simulating and testing the propagation channels of wireless communication systems [13]. In academia, [12] simulated a stochastic channel modeling under concise tunnel scenario, using the ray-tracing simulator, at the frequency of 30 GHz with 500 MHz bandwidth. Reference [14] used ray tracing tools to simulate the radio channel characteristics of the mobile hotspot network system in a typical linear subway tunnel in the 30 GHz band, and extracted and analyzed channel parameters for physical layer design. Reference [15] conducted a link simulation using a phased array model when using 28 GHz mmWaves at IAB-nodes, and studied the link performance of IAB-nodes affected by interference in the presence of other nearby IAB-nodes. In the industry,

3GPP TR 38.874 has introduced the IAB architecture that combines with the existing wireless networking architectures of operators, which can operate in SA or in NSA mode. There are two kinds of links in this architecture: backhaul link and user access link [10], and the reliability of the backhaul link is very important and sometimes the bottleneck of the wireless transmission [16], [17]. Reference [18] focus on the field trial of mmWave backhaul link in urban scenario for the vehicle at the speed of 60 km/h, and [19] conducted a field trial for mmWave backhaul link in subway scenario. Nevertheless, both papers do not specifically distinguish between the out of vehicle backhaul link and the in-vehicle user access link, which is essential for meeting user demand of internet access rates. Since mmWave, currently being used as wireless backhaul, will be newly applied for 5G user access [20], mutual interference occurs in the case of spectrum sharing between the user access link and the backhaul link. Focusing on the characteristics of mmWave, [21] used a new method to calculate the interference between the access link and the backhaul link in the case of spectrum sharing. To avoid interference, [17] utilize the approach of Time Division Multiplexing (TDM) + beam Space Division Multiplexing (SDM) for dynamic resource allocation on the access and backhaul links in the case of in-band IAB [10], and conducted field trials to test coverage and throughput. However, the disadvantage of this approach is that the large bandwidth resources of mmWaves are not fully utilized on the weak backhaul links at certain times, which is not suitable for the access of users in high-speed moving carriages.

For the 5G signal coverage inside the carriage, there are currently three ways to meet the data service needs of users in the carriage: macro station only, in-train repeater and IAB + small station. In the 4G era, the layout of macro stations is the main way to achieve signal coverage inside the carriage. Although users can access the network without any extra infrastructure on a train, penetration loss through metal carriage and signaling storm in a group handover [22] make the macro only layouts unsuitable for 5G signal coverage inside the carriage. To compensate penetration loss, with the advantage of small investment and a simple network, in-train repeaters have been applied to improve the quality of service for mobile users by European train operators for the time being [23]. Nevertheless, the overlapping coverage as well as the latency difference between repeater and the donor station cause interference, which leads to Signal to Interference Noise Ratio (SINR) deterioration after amplification [24]. Therefore, another scheme is exploited to overcome penetration loss: IAB + small station. In this method, the macro station acts as IAB-donor and will mainly communicate with the IAB-node at high data rates instead of communicating with a major number of small stations directly [3]. Therefore, the frequent handover burden of the train system can be significantly reduced, by conducting a group handover representing all the IAB-node associated small stations [1].

The disadvantage of this method is, if the same frequency band is used inside and outside the carriage for access link and backhaul link, the signal from IAB-donor will cause strong interference to the signal inside the carriage [16]. In this paper, a solution to this problem is proposed: Using different channels with different frequency bands for the access link and backhaul link inside and outside the carriage. The dual link of 4G commercial band + 5G mmWave is applied for the backhaul link outside the carriage and 5G commercial frequency band is applied for the in-vehicle access link of small station in the carriage. The small station performs as a picocell when serving the passengers in the carriage, and as a regular user when communicating with the macro station acting as an IAB-donor [25], which reduces the handover burden by conducting handover only for IAB-node instead of for all the passengers' terminals in the moving carriage. Moreover, For the case that mobile operators have collaborated on 5G RAN sharing, the 5G spectrum of different operators can be aggregated and shared together in one small station, so that the whole 5G frequency bandwidth of the operators can be fully used for user access in the carriage to match the mmWave large bandwidth of the backhaul link outside the carriage. Through the 5G RAN-sharing technology described in [26], which is applied in this new scheme, the users of all cooperative operators can access to in-vehicle small stations that aggregate 5G bands from all cooperative operators.

In order to take advantage of the 4G base stations already installed in the subway tunnel and save the cost of upgrading the core network from Evolved Packet Core (EPC) to 5G Core (5GC), we combine the IAB backhaul link to the 5G NSA architecture as suggested in [10]. By this means the continuous coverage of 4G low-frequency networks can provide IAB-nodes with control plane connection, while 5G mmWave mainly provides large bandwidth for user plane data transmission. Even if the mmWave link quality is seriously degraded because of the high-speed of the subway carriage as well as directional and narrow 5G mmWave beam [27], the IAB-node can still maintain the connection with the 4G master node and re-establish the mmWave link through the exchange of control information on the 4G low-frequency band. By means of Carrier Aggregation (CA), the bandwidth of up to 8 cells can be aggregated together for Frequency Range 2 (24.25 GHz-52.6 GHz), so the bandwidth of mmWaves in 5G base station is no longer limited to a single carrier of 400 MHz, which is the maximal bandwidth of one mm-Wave cell [28]. Presenting a field trial of this scheme and comparing the results with a similar field trial as well as empirical value using leaky cables, this scheme shows some advancement and can provide a reference for upgrading 4G to 5G signal coverage in all tunnel scenarios.

This paper aims to address the following issues: 1. Avoiding the penetration loss through IAB plus small stations. 2. Avoiding the signaling storm in a group handover that occurs at the base station on the tunnel wall for all the passenger users in the carriage, and each carriage can be

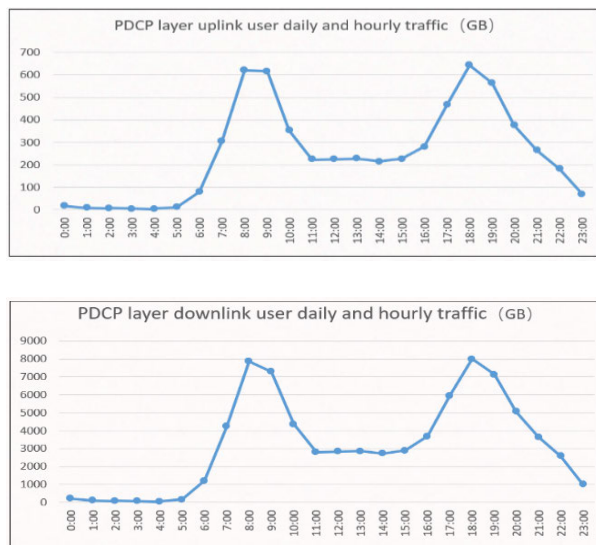


FIGURE 1. The average daily uplink and downlink flow of Shanghai subway.

handover as a whole between the IAB-nodes on the top of the carriage and the base station on the tunnel wall without the need to perform a group handover for all the users in the carriage, which simplifies the burden of the handover algorithm. 3. Adopting CA technology to expand transmission bandwidth. 4. The NSA architecture for the backhaul link not only utilizes the existing 4G devices, but also maintains the connectivity of 4G master node through cell merging during the 5G second node handover, which can quickly re-establish the mmWave link through the exchange of control information on the 4G low-frequency band.

The remainder of this paper is organized as follows. The background introduction to the current situation and challenges for the subway communication are given in Section II. Section III describes some technical problems related to mmWave transmission and railway tunnel communication. Section IV describes in detail the backhaul link integrated with the existing network, the in-vehicle small-station access link, and the overall network architecture of the whole scheme, as well as various capacity enhancement, handover reduction techniques and RAN-sharing techniques which are also incorporated in our scheme. In Section V, a field trial on Shanghai Metro Line 9 is carried out to verify the feasibility of the proposed scheme, providing the test results for both the backhaul link and the end-to-end access link for a subway carriage running of the speed of 80km/h. Finally, conclusions and future work are drawn in Section VI.

II. BACKGROUND INTRODUCTION

Under the traditional coverage method of leaky coaxial cables, the thick metal body of the subway causes signal attenuation, and the Doppler frequency offset caused by high-speed movement affects signal transmission and reception, posing greater challenges to network capacity during morning and evening peak periods, as showed in figure 1,

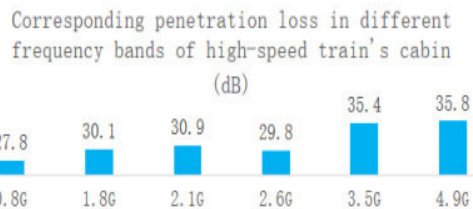


FIGURE 2. Penetration loss in different frequency bands.

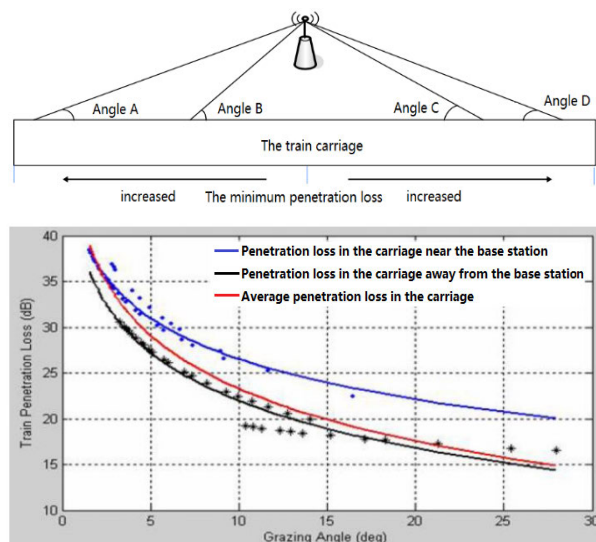


FIGURE 3. The relationship between train penetration loss and grazing angle.

which depicts the average daily uplink and downlink flow of Shanghai subway with time. A new approach is urgently needed to alleviate the pressure on network capacity and address the demand for large data volumes for passengers surfing the internet in subway carriages.

III. PROBLEM STATEMENT

In this section we analyze the problems faced by signal transmission in subway tunnel scenarios, with a focus on the characteristics of mmWaves and their suitability for propagation in tunnels, as well as the new design elements introduced by industry in terms of 5G standards for the characteristics of users traveling at high speeds.

A. PENETRATION LOSS

Figure 2 shows the measured corresponding penetration loss in different frequency bands of high-speed train’s carriage [16]. In general, the higher the frequency used in wireless communication systems, the weaker the penetration ability, so the penetration loss in the 5G frequency band (2.6 GHz-4.9 GHz) is higher than that in the previous 4G frequency band (0.8 GHz-2.1 GHz). Millimeter waves, which is in the high-frequency range, will have greater penetration loss compared to the commercial 5G bands mentioned above.

Another factor that affects penetration loss is the signal grazing angle: Figure 3 shows the relationship between

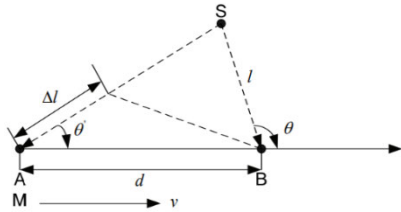


FIGURE 4. The additional phase increment $\Delta\phi$ due to the movement of the object.

grazing angle and penetration loss. The smaller the grazing angle, the greater the penetration loss, with the smallest penetration loss when the incident signal is perpendicular to the carriage body. Because the railway lines usually adopt a slender linear distribution, the angle between the base station signal and the carriage body (i.e., grazing angle) is usually small, which together with the closed carriage design increase signal loss. In subway tunnel scenario, due to the narrow space between the tunnel wall and the carriage, the grazing angle is even smaller than in open spaces.

Therefore, penetration loss is a major problem to be solved in 5G millimeter signal coverage in subway tunnel scenarios.

B. DOPPLER FREQUENCY OFFSET

High-speed movement will lead to severe signal reception variations, such as doppler offset, which causes performance deterioration of receiver demodulation. For doppler offset, the additional phase increment $\Delta\phi$ due to the movement of the object can be expressed by the equation:

$$\Delta\phi = 2\pi \Delta l / \lambda = 2\pi v \Delta t / \lambda \cos \theta \tag{1}$$

Thus, the value of doppler frequency offset can be derived, which is:

$$f_d = 1/2\pi \Delta\phi / \Delta t = v / \lambda \cos \theta \tag{2}$$

Then the relative frequency offset f_r is:

$$f_r = f_d / f = (v / \lambda) \cos \theta (c / \lambda) = (v / c) \cos \theta \tag{3}$$

In the straight tunnel environment, it could be supposed that $\theta \approx 0$ [29], it follows that:

$$f_r = \pm v / c \tag{4}$$

C in the above formula is the speed of propagation of a radio wave in the vacuum. Although the doppler offset in the tunnel is related to the frequency of the wave and the speed of the moving object due to the doppler effect, it can be seen that the relative frequency offset is only related to the speed of the moving object and not to the frequency of the wave [29].

For a vehicle travelling at 100 km/h in a tunnel, the maximum doppler offset of the 28 GHz wireless communication system is 2.59×10^3 Hz, and for any frequency band of radio waves, their relative frequency offsets are all 9.26×10^{-8} . Therefore, there will be no unbearable high doppler frequency offset in tunnel scenarios due to the high frequency

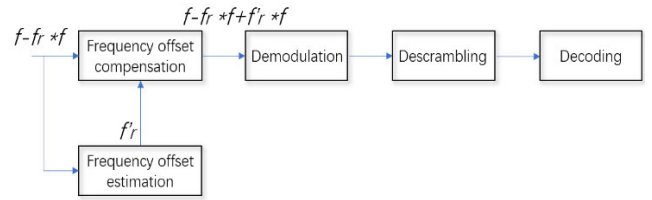


FIGURE 5. Frequency offsets correction process.

of mmWaves, so we can use conventional methods to compensate doppler frequency offset in this case.

In the 3GPP standard-defined 5G system, the phase difference between two adjacent Demodulation Reference Signal (DMRS) symbols in the time slot is used to calculate the corresponding frequency offset. In the OFDM system used in 5G, according to the 3GPP standard, the maximum frequency offset range that can be estimated for different frequencies and different Sub-Carrier Space (SCS) is:

$$\pm (\pi / 2\pi) \times \left(\frac{1}{\text{DMRS interval in time domain}} \right) \times \text{SCS} \tag{5}$$

Compared with the SCS of the current 5G commercial bands, mmWave's SCS is larger and can estimate a wider range of frequency offset, allowing for a wider range of frequency offset correction.

In order to better adapt to the rapid changes in channels in mobile user scenarios, additional DMRS has been added to 3GPP Release 16 in the frequency offset estimation step, allowing more DMRSs in the time domain to perform channel estimation (up to 3 additional DMRSs can be configured in the Physical Downlink Shared Channel (PDSCH) time domain), so that the terminal receiver can use these additional DMRSs for more accurate channel estimation [30].

In the industry, frequency offset estimation, frequency offset compensation, ICI cancellation, pilot configuration and other algorithms are introduced to quickly determine and compensate the frequency offset caused by high speed, as depicted in figure 5, which is conducive to improve the stability of wireless link and demodulation performance.

C. PATH LOSS

The path loss is affected by the transmission frequency and Pthe relative distance between the receiver and the transmitter. The higher the frequency of the radio wave, the shorter the wavelength, the weaker the diffraction ability, and the greater the loss during propagation. By and large, the path loss in free space decays exponentially with the increase of carrier frequency. To make up for it, the site density of 5G base stations should be greater than that of 4G base stations, which brings about large capital as well as operational expenditure for operators. However, different from the free space scenario, the radio wave propagation inside the tunnel for mmWave shows obvious regional characteristics. According to the two-stage model, the slope of path loss in the near-field region is very steep, while the waveguide effect appears in

the far-field region and the slope of path loss is significantly reduced [31]. The following formulas of the two-stage model are utilized to describe the path loss characteristics of radio propagation in tunnels [31]:

$$L_{dB} = L_0 + 10\gamma_1 \times \lg(d) \text{ if } d \leq R_b \quad (6)$$

$$L_{dB} = L_0 + 10\gamma_1 \lg(d_b) + \alpha^* (d - R_b) \text{ if } d \geq R_b \quad (7)$$

where L_{dB} is the path loss at a transceiver distance of d meters, L_0 is the path loss at a transceiver distance of d_0 meters, γ_1 is the exponential path loss index, α^* is the linear path loss factor, R_b is the location of the breakpoint, defined as the near-field region before the breakpoint and the far-field region after the breakpoint.

According to the power loss profiles of experimental and theoretical results for tunnel scenario in [31], the power of received signal attenuates sharply in the near field region, while in the far field region, the attenuation exhibits a linear and gentle characteristic, which indicates that, in the near-field region, the signal intensity fluctuates significantly due to the wave mode interactions of many higher-order modes, while in the far-field region, lower order wave modes play a dominant role, and the signal strength changes more smoothly. Moreover, as the distance between the transmitting and receiving antennas increases, the attenuation rate decreases [32].

As can be seen, using 5G mmWaves in a tunnel scenario, where the direction of the signal is concentrated and only covers the line of the tunnel, allows us to make full use of the advantages of mmWaves, such as large bandwidth, good directivity, low latency, etc., and at the same time, 5G stations do not have to be deployed as densely as in open space, thereby saving construction costs.

D. MULTIPATH PHENOMENA

As the signal propagates through the tunnel, in addition to direct waves, radio signals also generate multiple reflections on the tunnel walls, top and bottom, as well as diffraction when encountering obstacles. When the signals of each path reach the receiver for stacking, they will be enhanced due to same phase superposition and weakened due to opposite phase superposition, which will cause sharp fluctuations in the received signal amplitude and lead to multipath fading of the signal.

The synthetic signal received by the receiver is the superposition of the radio wave signals of each path from different directions and arriving at the receiver at different times. Therefore, the final received synthetic signal includes not only the signal from the direct path, but also the delay signal from multiple paths, which causes the signal received by the receiver to be stretched in time compared to the signal actually sent by the transmitter. This phenomenon is called delay spread.

If the transmitter sends a pulse signal $\delta(t)$, The signal received by the receiver will be composed of multiple pulse

signals with different time delays, namely:

$$h(t) = \sum_{i=1}^K e^{j\theta_i} \beta_i \delta(t - \tau_i) \quad (8)$$

where K is the number of pulses and τ_i is the delay of the i -th path. The value of K , τ_i and β_i will change with the movement of the mobile station.

The consequence of delay spread is: from the perspective of frequency domain, delay spread will lead to frequency selective fading of signals. In the process of signal transmission, on the one hand, due to the existence of delay spread, one symbol of the received signal will be extended to other symbol periods, resulting in Inter Symbol Interference (ISI), which will seriously reduce the transmission quality of the signal. In order to solve this problem, during transmission, the symbol period should be greater than the maximum delay spread T caused by the multipath effect or the symbol rate should be less than $1/T$ to reduce the possibility of ISI. On the other hand, for spread spectrum communication systems, if the relative delay between two multipath signals exceeds the pulse width of a spread spectrum code chip, the two multipath signals are uncorrelated and separable. Spread spectrum systems can use diversity techniques to separate or combine multipath signals to avoid ISI, thereby improving the quality of signal transmission.

Correlation bandwidth is another parameter related to delay spread, which can be used to determine whether the channel is a frequency selective fading channel or a flat fading channel, or to determine whether two signals are suitable for frequency diversity reception. Generally, the reciprocal of the symbolic bit period T_m is used to specify the relevant bandwidth B_c , i.e., $B_c = 1/T_m$.

For a digital system, in the absence of diversity techniques and balancing technique, the ratio of the root-mean-square time-delay spread σ_τ to the T_m must be less than 0.2, so that the ISI at the receiver can be tolerated [33], so B_c can be set to be approximately equal to $1/(5 \times \sigma_\tau)$. The following formula is usually used to describe σ_τ :

$$\sigma_\tau^2 = \frac{1}{G} \sum_{i=1}^K \tau_i^2 \beta_i^2 - (\bar{\tau})^2 \quad (9)$$

$$\bar{\tau} = \frac{1}{G} \sum_{i=1}^K \tau_i \beta_i^2 \quad (10)$$

$$G = \sum_{i=1}^K \beta_i^2 \quad (11)$$

According to [29], in the mine environment with obstacles, σ_τ is not larger than 103 ns, so that $B_c \approx 1/(5 \times \sigma_\tau)$ When there is no obstacle, σ_τ is not more than 22 ns, and B_c is close to 10MHz. While 5G mmWave adopts OFDM technology, the transmission signal subcarrier spacing is usually set to 120KHz at present, so this subcarrier bandwidth is usually within the B_c of the tunnel environment.

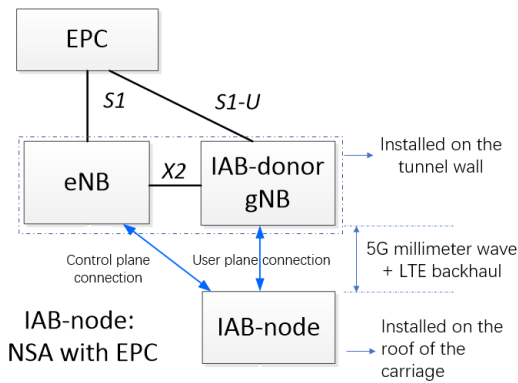


FIGURE 6. Backhaul link architecture.

IV. PROBLEM SOLUTION AND PROPOSED APPROACH

In this paper we design a new approach to meet the high data volume internet access of users in subway scenario, which is described in three aspects in this section: 4G + 5G mmWave Dual Connection (DC) backhaul, in-vehicle mobile user access, and overall network architecture. NSA architecture, cell merge of master node, Carrier Aggregation (CA), and beam forming technologies are applied to backhaul link to obtain stable user control plane connection, smaller handover latency, greater bandwidth, and more concentrated signal energy. In view of the user plane of the backhaul link using mmWave transmission, the current commercial frequency band can be fully utilized for the in-vehicle mobile user access, without having to allocate a portion for the backhaul link. The overall network architecture depicts the relationship between the whole system and the bearing network, core network and management platform.

A. DESIGN OF 4G+5G MMWAVE DUAL-CONNECTION BACKHAUL

1) IAB-NODE OPERATING IN NSA WITH EPC

Considering many subway tunnels have been previously deployed with evolved Node B (eNB, i.e., 4G base station), if all eNBs are abandoned and replaced with the next Generation Node Bs (gNB, i.e., 5G base station) and the EPC is replaced with 5GC, the cost will be high. In order to meet the high data volume as well as balancing system reliability and costs control at the same time, we combine the IAB backhaul link to the 5G NSA architecture as depicted in figure 6:

The IAB donor, acting as a secondary node, is a node that offers a UE interface to the core network, as well as wireless backhauling functionality to IAB-nodes, which can serve as a relay node to expand the coverage of IAB donors. The IAB-node installed on the roof of the carriage is dual connected to the existing eNB, which acts as a Master Node (MN), and the newly installed mm-Wave gNB, which forms a backhaul link between the tunnel wall and the subway carriages. In this way, the continuous coverage of 4G low-frequency of eNB can provide IAB-node with control plane connection, which can also be used for communication during system maintenance. At the same time, 5G mmWave mainly

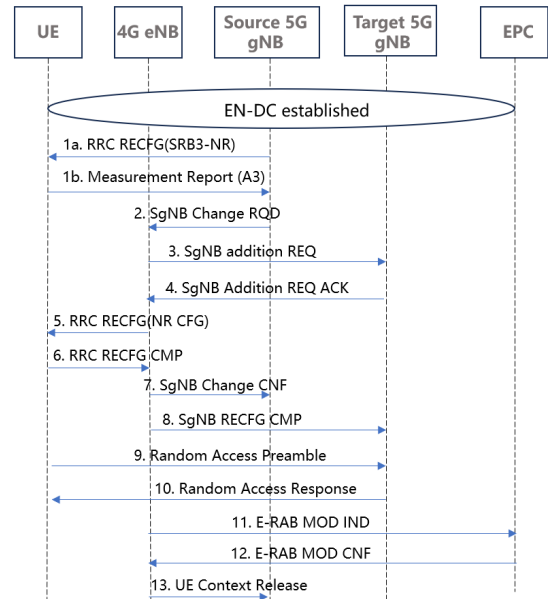


FIGURE 7. Processes for handover between EN-DCs: LTE(MN) does not handover, only NR(SN) hands over.

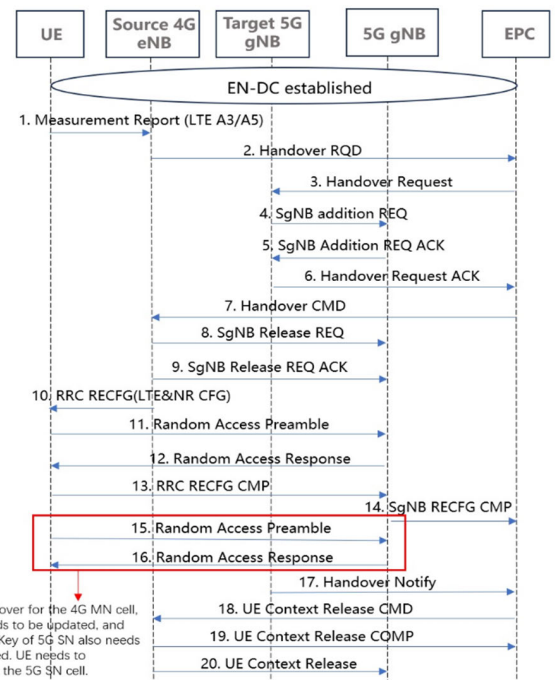


FIGURE 8. Processes for handover between EN-DCs: NR(SN) does not handover, only LTE(MN) hands over.

provides large bandwidth user plane data transmission to meet the high data volume internet access of passengers.

2) CELL MERGE FOR MASTER NODE

Since the signal coverage of MN and SN in the NSA architecture are different, due to different frequency bands they utilize, we summarize cell handover under dual connection into three cases: 1. MN remains unchanged while SN changes; 2. MN changes, SN remains unchanged; 3. Both

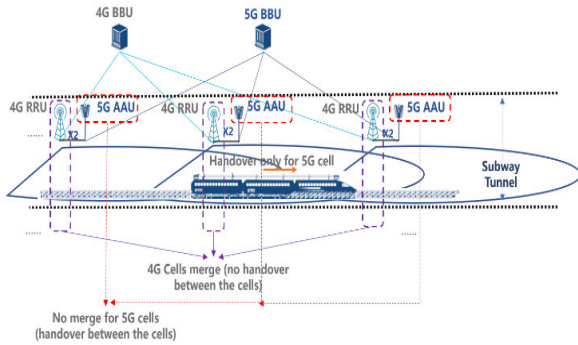


FIGURE 9. In the dual connection, 4G cells are merged, while 5G cells are not merged.

MN and SN change simultaneously. According to the handover process defined by 3GPP and the current network test experience, for the second case, although SN remains unchanged when MN changes, there are still processes for UE to reconnect SN, as shown in figure 8.

Comparing figure 7 and figure 8, it can be seen that although NR (SN) remains unchanged, only LTE (MN) handover takes more steps than only NR (SN) handover. Hence MN changes have the greatest impact on handover latency. Therefore, keeping MN without handover and only handing over between SNs is beneficial to reduce the handover latency.

In communication scenarios with high-speed mobile users, due to the short time that mobile users pass through the cell, frequent inter cell handover occurs, seriously affecting communication quality. Cell merge can solve the problems. By using optical fiber, the baseband signals of n Radio Remote Units (RRUs) installed at different base station sites are concentrated on a BBU (Base Band Unit), through which the original cells are merged into one cell, so that the coverage of the original cell is expanded by n times, and no handover occurs within this coverage. The cost of cell merge is bandwidth. When there is no cell merge, users in each original cell can use all the bandwidth of their own cell respectively. After cell merge, all users in the merged cell can share the bandwidth of only one original cell. In this paper, MN and IAB-node only have control plane signaling interaction and do not divert 5G traffic from SN. Therefore, without sacrificing any bandwidth for transmitting user data, we can merge MN cells together to reduce the impact of MN handover on latency. In the field trial of this paper, all MN cells are merged into one cell, so the control plane channel is uniformly scheduled, reducing handover, improving user perception, while the user plane channels of SNs are independently scheduled to meet the high-capacity requirements.

3) MILLIMETER WAVE CARRIER AGGREGATION

Dual connection (DC) and Carrier aggregation (CA) can be implemented together, especially to make full use of the large bandwidth of mmWave. Although the maximum bandwidth of mmWaves within a cell defined in the 3GPP Release 16 is 400MHz, the bandwidth can still be expanded through CA.

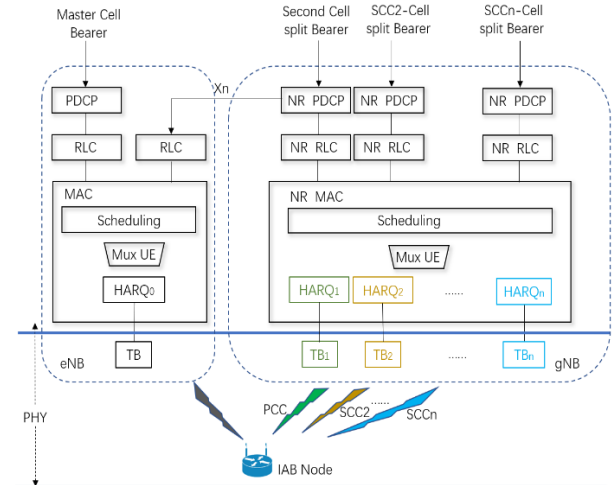


FIGURE 10. NSA Option 3x+CA for gNB.

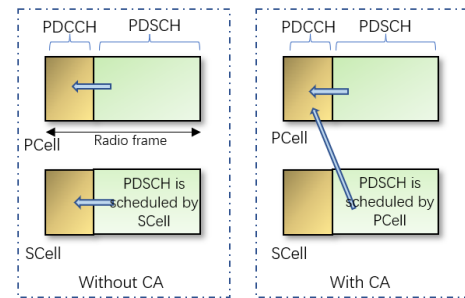


FIGURE 11. Scheduling of PDSCH with and without CA.

The figure 10 shows the network protocol architecture diagram using Option 3x NSA plus CA on gNB. In E-UTRAN New Radio Dual Connectivity, the user area traffic is allocated between eNB and gNB through the PDCP layer. Part of user plane data can be split-flowed from gNB to eNB through Xn interface, when the shunt switch of the Xn interface is turned on. In EN-DC, the terminal (IAB-node) has two C-RNTI: one for the Master Cell (MC) and another for the Secondary Cell (SC); It has one always active cell in MC and another always active cell in SC; MC and SC have their own independent Physical Downlink Control Channel (PUCCH) resources at the physical layer.

In our scheme, secondary cell and other cell carriers in the same gNB perform CA, which is implemented at the MAC layer. The SC carrier in the double connection is also the Primary Component Carrier (PCC) for PCell, and the other cells with CA are SCells with respective Secondary Component Carriers (SCC). Each component carrier occupies a separate HARQ process and L1 layer. Each subcarrier can use independent link adaptation technology to transmit data without affecting each other. In practice, the base station will select proprietary modulation and coding scheme for different subcarriers according to the channel quality difference of different subcarrier links.

At the physical layer, the Physical Downlink Control Channel (PDCCH) of the PCC Downlink Control Information

(DCI) contains information about the carrier resource blocks of not only the PCC but also the SCC, which can assist the base station in making resource scheduling decisions, thus realizing the PDSCH allocation of PCell and all SCells. The implementation principle is depicted in figure 11.

4) MILLIMETER WAVE BEAMFORMING FOR TUNNEL BACKHAUL SCENARIO

Although mmWave signals can achieve high spectral efficiency, they have high losses in the air, poor penetration ability, and difficulty penetrating obstacles on the propagation path [34]. These characteristics determine that in order to apply mmWave technology to more general scenarios, 5G systems must combine beamforming technology into it.

High diversity gain can be obtained by using large-scale antenna arrays, which can overcome the path loss of mmWave and expand the coverage. Beamforming technology can further improve antenna efficiency, compensating for the shortcomings of mmWave communication such as high path loss and small coverage. Using the mmWave band, the physical size of the antenna array and associated electronics can be further reduced, allowing more antenna units to be installed in the same physical space. The reduction in the size and the increase in the number of antenna-related components also in turn increase the adjustable dimension of beam shaping.

In this paper we use mmWave single beam assignment for the gNB cell, because if it is configured as multiple CSI-RS beam, high-speed moving terminals may need frequent beam realignments when moving between beams, which may continuously lead to high feedback overhead. In addition, call drop rates will rise if the beam is not switched in time during high-speed movements of terminals.

However, due to the dual-link architecture of backhaul, in addition to the directional and narrow mmWave beam, whose energy is concentrated, there are also the wide beam of 4G low-frequency for the MN cell of NSA, which can maintain the connection with the eNB and re-establish the mmWave link through the exchange of control information on the 4G low-frequency band, when the mmWave link quality is seriously degraded.

B. THE DESIGN OF IN-VEHICLE MOBILE USER ACCESS THROUGH SMALL STATION

The distributed small base station consists of BBU, Remote HUB (RHUB) and Pico RRU (pRRU). The signal source is the BBU, that is connected to the RHUB. The digital baseband signal is transmitted through the Common Public Radio Interface (CPRI) interface, and then transmitted through the network cable to the pRRU at the end, which converts it into an RF signal for transmission. The indoor distributed system has the characteristics of simple structure, fewer nodes, small size, light weight, convenient device connection, convenient expansion, and flexible deployment.

Unlike the traditional method of outdoor signal penetrating indoors, the vehicle-mounted indoor distributed system

designed in this paper, are connected to the vehicle mounted backhaul system, and then dual-connected wirelessly to the NSA base station installed on the tunnel wall through the roof antenna installed in the IAB-node. In this way, the traditional method of outdoor signal penetrating indoors is changed to a backhaul link outside the carriage and a user access link inside the carriage, thus avoiding the penetration loss, as shown in module 1 and 2 in figure 12. The operator's existing 5G commercial frequency band is applied for the access link, while the 4G commercial frequency band plus 5G mmWave frequency band are applied in the dual-connection between the in-vehicle IAB-node and NSA base station on the tunnel for backhaul link.

In view of the situation that some operators use RAN sharing to reduce investment as well as operating expenses, there are two types of small stations applied in this paper: a non-shared station (small station 1), which can only be accessed by users of one operator, and a shared station (small station 2), which can be accessed by users of multiple cooperative operators. The RAN-sharing technology adopted by the shared station is Multi Operator Core Network (MOCN), in which the Public Land Mobile Network (PLMN) Identities (IDs) proprietary to different operators are broadcasted in System Information Block 1 (SIB1) simultaneously [26] and each operator has its own independent logical cells [35].

C. OVERALL NETWORK ARCHITECTURE DESIGN

Figure 12 depicts the overall network architecture of the vehicle ground backhaul system utilized in this paper. The system consists of in-vehicle active indoor distributed system, vehicle backhaul system, tunnel backhaul system, the reused existing bearing network and vehicle-ground backhaul management platform, in which the in-vehicle active indoor distributed system and vehicle backhaul system are already introduced in the previous section. The tunnel backhaul system can be seen as a base station installed on the tunnel wall. A set of backhaul CU and DU connects multiple.

Active Antenna Units (AAUs), which can be connected to IAB-nodes installed in different carriages through mmWave communication. The in-vehicle active indoor distributed system, vehicle backhaul system and tunnel backhaul system belong to the wireless communication system, which is not so reliable, and has a high probability of retransmission, so they are the focus of the field trial in this paper.

Due to the NSA architecture for the backhaul link in the tunnel, the tunnel backhaul system connects to the 4G core network (EPC), and the bearer network can leverage the previous 4G bearer network. The vehicle-ground backhaul management platform is in charge of not only the management of tunnel backhaul system and vehicle backhaul system, involving parameter configuration and status monitoring, but also the on-board users, chiefly including controlling user registration, user information management, user access management, user data forwarding, user network policy management and session management [36].

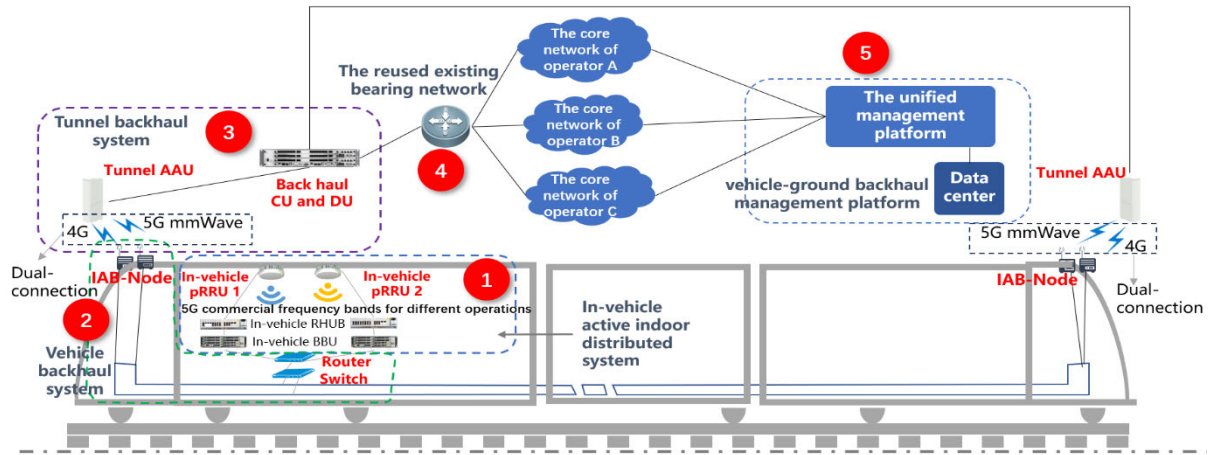


FIGURE 12. Overall network architecture design.

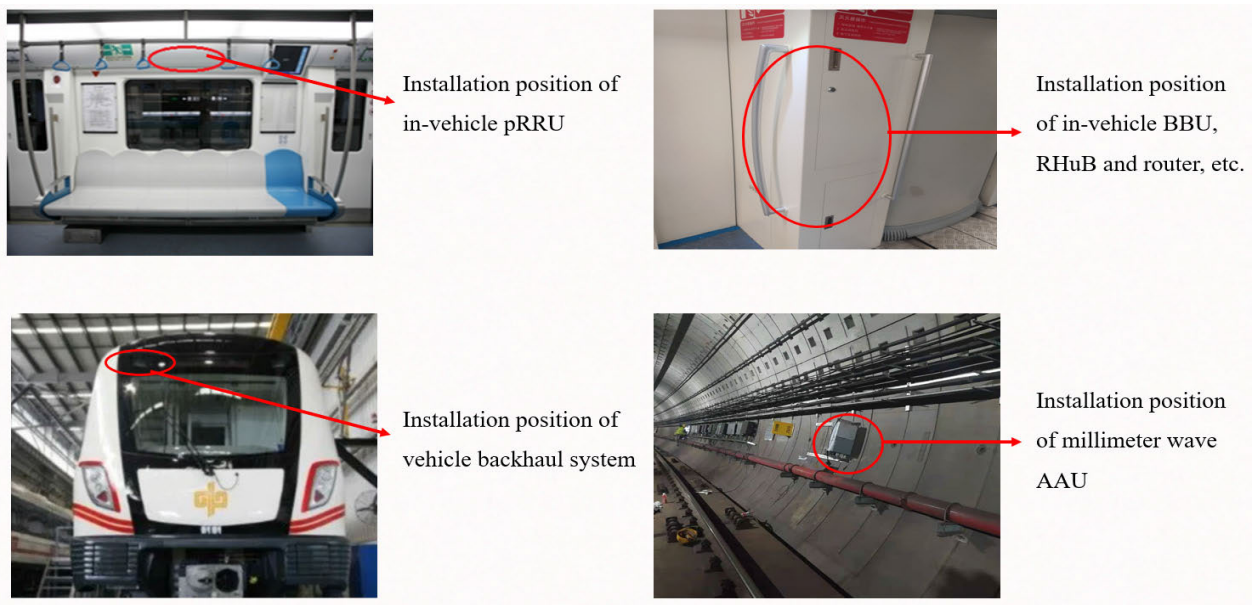


FIGURE 13. Equipment installation location.

V. EXPERIMENTAL AND RESULTS OF FIELD TRIALS

A. THE TESTS FOR DUAL-CONNECTION BACKHAUL LINK

Millimeter wave usually refers to the frequency bands at 30–300 GHz, but researchers also prefer to add the nearby centimeter frequency bands from 24 GHz to 28 GHz in discussion. In our field trial, the frequency band used for mmWave is 26.2–27.0 GHz, with 4×200 MHz bands for carrier aggregation and a total bandwidth of 800 MHz. The parameters of backhaul link are displayed in table 1.

Figure 13 shows the pictures of the installation location of in-vehicle equipment and mmWave AAU. The total length of the test tunnel is 6.5 km, of which there are 1200 m complex scenarios such as line of sight (LOS) environment (within 150 m), continuous S-curves (the first one is 200 m long, the second one is 400 m, the third one is 500 m) and with up and down slope (length 800–1000 m) in the tunnel. Therefore, this

test tunnel is very typical and can basically cover most of the tunnel scenarios.

1) MILLIMETER WAVE COVERAGE TEST IN SUBWAY TUNNEL a: BASE STATION REMOTE TEST

Remote test is helpful for subsequent base station deployment planning. Taking IAB-node's RSRP = -95 dBm as the target coverage, and conducting experiments on the most complex railway section, we confirmed through tunnel coverage tests that the 26 GHz mmWave coverage capability is 680 m, as shown in figure 14.

At present, the distance between commercial 5G base stations in the 3.5 GHz frequency band is usually set at around 650 m in general urban areas. Due to the high frequency band, if mmWave base stations are deployed in urban areas on the ground, the station spacing should be much less than

TABLE 1. Parameters of backhaul link.

PARAMETERS	VALUE
The cells of anchor eNB	11
IAB-node	1
4G Frequency range	1920-1940/2110-2130 MHz
The cells of 5G Donor base stations	11
5G Frequency range	26.2 ~27.0 GHz
Carrier bandwidth	200 MHz
DL Number of Carrier	4
UL Number of Carrier	2
Wave form	OFDM
Subcarrier spacing	120 kHz
Slot length	0.125 ms
Symbols/slot	14
TDD-UL-DL-Pattern	DDDSU
The number of antenna units for 5G Donor base station	512
The number of transmitter and receiver of 5G Donor base station	4T4R
Output power of 5G Donor base station	39 dBm

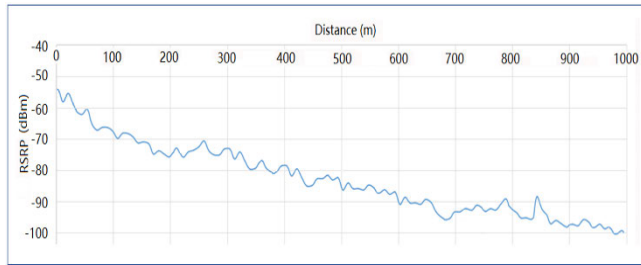


FIGURE 14. Received RSRP for Terminal of backhaul link vs distance.

650 m. However, due to the waveguide effect of mmWave, as discussed in Section I of this paper, the spacing between 5G mmWave base stations in tunnel scenarios is much greater than its deployment on the ground, which to some extent proves that mmWaves are suitable for communication in tunnels.

We combine the field trial results displayed above and environmental investigation to confirm the preliminary location of the installation of tunnel equipment and in-vehicle equipment.

b: TERMINAL RECEPTION LEVEL FOR STRAIGHT AND CURVED TUNNEL

For Straight Tunnel: In this field trial, we compared the terminal receiving levels in free space and in straight tunnel. The results are shown in figure 15.

Comparing with the reception level of the terminal in free space, the in tunnel measured reception level of the terminal has been consistently higher than that of the free space propagation, and the rate of decline has gradually slowed down with distance, indicating a typical waveguide effect in the tunnel.

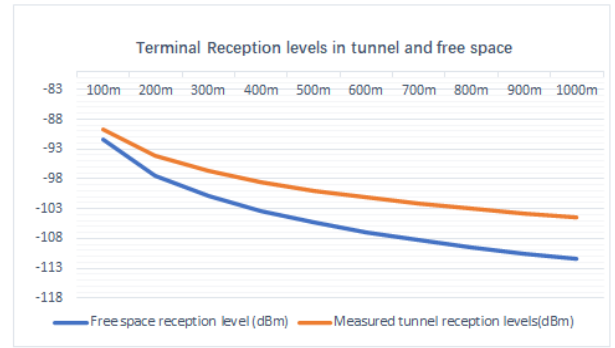


FIGURE 15. The terminal receiving levels in free space and in straight tunnel.

TABLE 2. The terminal receiving levels at distance of 800m from the mm-Wave station in straight and curved tunnels.

At the distance of 800m	Straight tunnel	Curved tunnel
curvature = (1/3000 m)	-102.98 dBm	-107.52 dBm
curvature = (1/1500 m)		-110.35 dBm
curvature = (1/800 m)		-114.21 dBm
curvature = (1/400 m)		Expected value <122 dBm

For Curved Tunnel: Millimeter waves mainly rely on straight line of sight propagation, and when a tunnel bends, it has a significant impact on its transmission power and latency. In this paper the subway tunnel for the field trial has straight tunnel sections and curved tunnel sections. Curved tunnels increase the number of wave reflections, which are the most important part of wave propagation losses in tunnels, and more precisely, the radio propagation loss is proportional to the curvature of the tunnel: the greater the curvature the more detrimental to signal propagation.

Table 2 shows the terminal receiving levels at distance of 800 m from the 5G mmWave station in curved tunnels with different curvature.

At the same distance, the reception level of a curved tunnel will be lower than that of a straight tunnel, with weaker signal coverage, which results in greater fluctuations in terminal data rates when handing over between cells in curved tunnels than in straight tunnels, which is reflected in more dense troughs of data rates on the time axis in figure 16-18. The station deployment will be slightly denser, but it should not be too dense because in this way there will be inter-cell signal interference for the same frequency networking.

2) THE DATA THROUGHPUT OF A MOVING IAB-NODE

In this field trial we tested the data throughput of the backhaul link for a moving IAB-node, which is installed on a subway carriage travelling at 80 km/h. With the downlink and uplink data throughput showed in figure 16 and figure 17, we can see the performance of the backhaul link.

Through packet filling test from the core network to the mobile IAB-node, we can obtain the downlink throughput of the backhaul link, which is 3.6 Gbps on average and

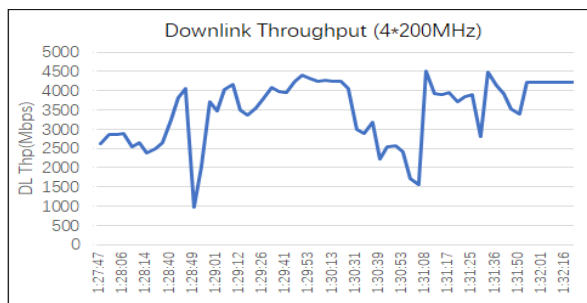


FIGURE 16. Downlink throughput for 4 x 200MHz CA for backhaul.

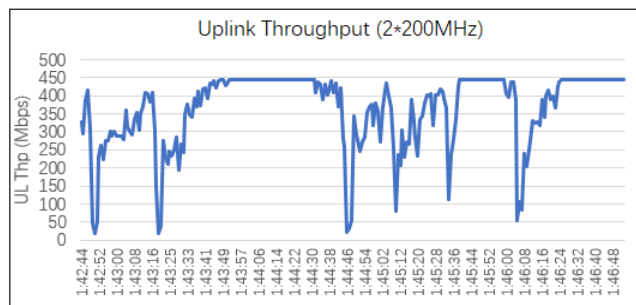


FIGURE 17. Uplink throughput for 2 x 200MHz CA for backhaul.

4.5 Gbps at maximum. Since all cells of 4G master node in NSA are merged, there is no handover for the cells of 4G master node, and only NR cells change. Since 4G master node uses relatively low frequency and covers a farther distance than 5G mmWave, at least the control plane between the 4G master node and the IAB-node is not affected by handover, which explains the impact on the downlink throughput is not so significant in the test: Under 4 x 200 MHz carrier aggregation, the lowest rate at the handover point is still 1 Gbps, which does not affect user perception. The figure 16 shows a section of curves with gentle fluctuations and a section with significant fluctuations, corresponding to the straight tunnel section and the curved tunnel section, respectively.

In the case of 2 x 200 MHz carrier aggregation, the average uplink throughput of backhaul link is 360 Mbps, and the highest uplink throughput reaches to 447 Mbps. Due to the limited power of IAB-node, the uplink is more sensitive to the handover point. Despite this, the handover latency is only over 100 milliseconds, which has actually little impact on the user perception and average rate throughput. However, due to weak signal coverage and fast fading in curved tunnels, when IAB-nodes move at a relatively high rate in curved tunnels, the angle between the line connecting the receiver and the wave source and the velocity direction is no longer approximately 0, resulting in a larger doppler frequency offset, which causes the uplink throughput for the backhaul link of the curved tunnel area to fluctuate greatly at the handover point. However, the minimum throughput of the uplink handover point is still greater than 14 Mbps, and rebound quickly after the handover point.

TABLE 3. Parameters of the access link in the carriage.

Frequency band	3.5 GHz	2.6 GHz
Frame Structure	DDDSUDDDSU	DDDSUDDDD
Special subframe time slot ratios	10:2:2	6:4:4
Bandwidth	100 MHz	100 MHz
Test Terminal	commercially available 5G terminal	commercially available 5G terminal

TABLE 4. The peak and average data throughput of the end-to-end access link.

Frequency band	Theoretical peak throughput	Measured peak throughput	Measured average throughput
3.5 GHz	DL:1.5 Gbps	DL: 1.2 Gbps	DL: 870 Mbps
	UL:350 Mbps	UL: 249 Mbps	UL: 178 Mbps
2.6 GHz	DL:1.7 Gbps	DL: 1.39 Gbps	DL: 1.04 Gbps
	UL:264 Mbps	UL: 261 Mbps	UL: 202 Mbps

B. ACCESS LINK IN THE CARRIAGE

In the field trial of the in-carriage access network, the performance of the operator’s commercial access network in the carriage traveling at 80 km/h can be tested to verify the feasibility of the whole solution from end-to-end. Taking into account both the adopted and unadopted RAN sharing scenarios, the small stations in the carriage have access to 100 MHz of bandwidth in each of the 2.6 GHz and 3.5 GHz bands, with the 2.6 GHz band being accessed by a single operator, while the 3.5 GHz band enables shared access for two operators. The specific parameters of the access link in the carriage are shown in the following table:

The peak and average UL/DL data throughput of the end-to-end access link for 3.5 GHz and 2.6 GHz frequency bands are shown in the table 4:

Due to the limited power of mobile terminal, it can also be seen from the backhaul test that the uplink performance is usually not as good as the downlink. Therefore, we focus on the data rate performance of uplink access link in the carriage and draw the data throughput curve with time. If the uplink performs well, the feasibility of the whole scheme from end to end can be verified.

The test results of the access network of the small station inside the carriage are shown in the figure 18. In the curved tunnel section, the uplink throughput fluctuates a bit more dramatically, which is consistent with the uplink performance of backhaul link. At some handover points, the uplink rate throughput decreases to 8-9 Mbps, but rebounds quickly, which does not have a significant impact on the uplink service and the user perceives no difference.

VI. EXPERIMENTAL RESULTS DISCUSSION

A. FOR BACKHAUL LINK

The results of UL/DL backhaul link data throughput go beyond previous reports of similar field trial in [37], showing that around 1.25 Gbps / 110 Mbps of DL/UL throughput are achieved with bandwidth of 500MHz. Assuming that the bandwidth was 800 MHz, the DL/UL throughput would be roughly 2 Gbps / 176 MHz, which is obviously lower than the

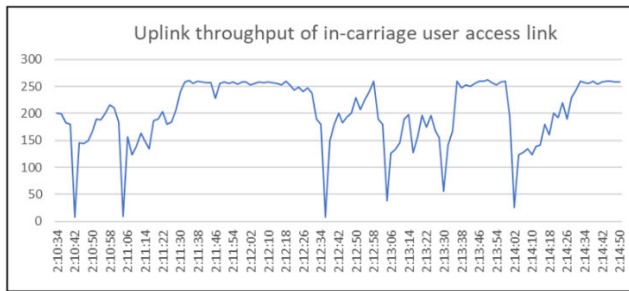


FIGURE 18. Uplink throughput for access network of the in-carriage small station.

average DL/UL throughput of 3.6 Gbps / 360 Mbps resulting from the field trial in this paper.

B. FOR ACCESS LINK IN THE CARRIAGE

The DL/UL peak throughput measured in the carriage reaches to 1.39 Gbps / 261 Mbps, and the DL/UL average throughput reaches to 1.04 Gbps / 202 Mbps. Comparing to the empirical value using current leaky cables, whose DL/UL average throughput is 600 Mbps / 93 Mbps for 5G and 42Mbps / 15Mbps for 4G in the carriage, the test results of end-to-end access link using the new scheme showed significant improvement.

However, some data throughput troughs occurred at the time point of handover. From the results of the field trial, it can be seen that the throughput troughs are caused only by the handover of the backhaul link, not by the small station inside the carriage, so using small stations for user access does not have any adverse effects on handover, only the handover for backhaul link is still not very stable and need to be improved. However, due to the 4G connection in the control plane, the minimum downlink throughput for backhaul link is still more than 1Gbps, and the minimum uplink throughput is more than 14Mbps. Although the throughput troughs rebound quickly, which does not have a significant impact on the service and the user perceives no difference, further optimization for handover is still needed to enhance the user experience.

VII. CONCLUSION

With the development of mobile communication technology, higher frequency bands are being exploited, and mmWaves will be likely used to satisfy the increasing data rate requirement. Millimeter waves, which is in the high-frequency range with short wavelength and large bandwidth, are suitable for the subway tunnel scenarios. In order to overcome the handover burden and penetration loss of mmWave, that is more significant in the high-frequency range, the scheme of IAB + small station is proposed in this paper, whose wireless transmission can be divided into 4G commercial frequency band + 5G mmWave dual link for backhaul and 5G commercial frequency band access link in the carriage. By this means, each carriage can be handed over as a whole between the IAB-nodes on the top of the carriage and the base station on

the tunnel wall, and all the passenger users' handovers occur in the small stations installed in the carriages. NSA architecture, cell merging and carrier aggregation technology were applied to the backhaul link, which could realize equipment reuse, reduce handover latency, increase wireless bandwidth and improve data throughput. Through RAN-sharing technology, the 5G frequency bands of cooperative operators are aggregated in one small station and fully used for user access to match the mmWave large bandwidth of the backhaul link. We conducted field trials for this scheme in a complex scene with straight and curved tunnels, and analyzed the backhaul link and access link separately. The test results showed that the problem of penetration loss was solved, the data throughput has been greatly improved by the CA of backhaul link (the end-to-end peak throughput in the carriage reached to 1.39 Gbps for downlink and 261 Mbps for uplink), and there were always 4G connection at the time point of handover, due to cell merge of 4G MNs.

VIII. FUTURE WORK

Nevertheless, this scheme still has much to be improved., such as better adaptation between the backhaul module and small station to reduce throughput loss, optimization of mmWave beam forming, etc. Among them, the most important one is the handover optimization, which aims to make the data throughput to perform more smoothly when handing over and the user experience better.

Aiming at this problem, the existing research is mainly divided into two categories: physical layer-based handover optimization algorithm and high-level-based handover optimization algorithm. The physical-layer based handover algorithm mainly aims to achieve fast handover and optimal signal reception quality by optimizing physical layer parameters, such as channel access threshold, received signal-to-noise ratio, etc. However, this method requires a significant amount of time and resources, and is not practical enough. The high-level-based handover optimization algorithm is mainly to predict the next position of the mobile terminal through accurate prediction algorithm, so that the terminal can handover to the most suitable base station in time during the movement. Based on the characteristics of subway track driving, whose driving route is relatively fixed, this algorithm is very suitable for subway communication, so it will be the focus of our future work.

REFERENCES

- [1] G. Noh, B. Hui, and I. Kim, "High speed train communications in 5G: Design elements to mitigate the impact of very high mobility," *IEEE Wireless Commun.*, vol. 27, no. 6, pp. 98–106, Dec. 2020.
- [2] *Service Requirements for the 5G System*, 3GPP, document TS22.261, 2021.
- [3] C.-X. Wang, A. Ghazal, B. Ai, Y. Liu, and P. Fan, "Channel measurements and models for high-speed train communication systems: A survey," *IEEE Commun. Surveys Tuts.*, vol. 18, no. 2, pp. 974–987, 2nd Quart., 2016.
- [4] H. Miao and L. Xiong, "Channel characteristics of subway station based on ray-tracing at 5G mmWave band," in *Proc. IEEE/CIC Int. Conf. Commun. China (ICCC)*, Chongqing, China, Aug. 2020, pp. 687–692.
- [5] L. Xiong, H. Miao, B. Ai, T. Juhana, and A. Kurniawan, "Channel characteristics of high-speed railway station based on ray-tracing simulation at 5G mmWave band," *Int. J. Antennas Propag.*, vol. 2019, pp. 1–10, Sep. 2019.

- [6] Y. Liu, C.-X. Wang, A. Ghazal, S. Wu, and W. Zhang, "A multi-mode waveguide tunnel channel model for high-speed train wireless communication systems," in *Proc. 9th Eur. Conf. Antennas Propag. (EuCAP)*, Apr. 2015, pp. 1–5.
- [7] *Technical Specification Group Radio Access Network; Study on Self-Evaluation Towards IMT2020 Submission*, 3GPP, document TR 37.910, 2019.
- [8] *Technical Specification Group Radio Access Network NG-RAN Architecture Description*, 3GPP, document TS 38.401, 2022.
- [9] *Ericsson Microwave Outlook 2018*, Ericsson, Stockholm, Sweden, Dec. 2018.
- [10] *Technical Specification Group Radio Access Network; NR; Study on Integrated Access and Backhaul (Release 16)*, 3GPP, document TR 38.874, 2019.
- [11] G. Ke, A. Bo, and H. D. Ping, "Towards smart rail mobility at the mmWave and THz bands: Challenges, solutions, and future directions," *Sci. Found. China*, vol. 2020, pp. 1–12, Jan. 2020.
- [12] K. Guan, J. Moreno, B. Ai, C. Briso-Rodriguez, B. Peng, D. He, A. Hrovat, Z. Zhong, and T. Kurner, "5G channel models for railway use cases at mmWave band and the path towards terahertz," *IEEE Intell. Transp. Syst. Mag.*, vol. 13, no. 3, pp. 146–155, Fall 2021.
- [13] J. D. V. Sánchez, L. Urquiza-Aguiar, and M. C. P. Paredes, "Fading channel models for mm-wave communications," *Electronics*, vol. 10, no. 7, p. 798, Mar. 2021.
- [14] G. Li, B. Ai, K. Guan, R. He, Z. Zhong, B. Hui, and J. Kim, "Channel characterization for mobile hotspot network in subway tunnels at 30 GHz band," in *Proc. IEEE 83rd Veh. Technol. Conf.*, Nanjing, China, May 2016, pp. 1–5.
- [15] T. Inoue, "5G NR release 16 and millimeter wave integrated access and backhaul," in *Proc. IEEE Radio Wireless Symp. (RWS)*, Jan. 2020, pp. 56–59.
- [16] X. Zhao, Z. Li, C. Hu, and J. Hou, "Solutions of 5G RAN on high-speed train," in *Proc. 5th Int. Conf. Commun. Eng. Technol. (IC CET)*, Shanghai, China, Feb. 2022, pp. 949–953.
- [17] T. Tian, Y. Dou, G. Ren, L. Gu, J. Chen, Y. Cui, T. Takada, M. Iwabuchi, J. Tsuboi, and Y. Kishiyama, "Field trial on millimeter wave integrated access and backhaul," in *Proc. IEEE 89th Veh. Technol. Conf.*, Apr. 2019, pp. 1–5.
- [18] H. Chung, J. Kim, G. Noh, B. Hui, I. Kim, Y. Choi, C. Choi, M. Lee, and D. K. D. Kim, "From architecture to field trial: A millimeter wave based MHN system for HST communications toward 5G," in *Proc. Eur. Conf. Neww. Commun. (EuCNC)*, Jun. 2017, pp. 1–5.
- [19] J. Kim, H. Chung, G. Noh, B. Hui, I. Kim, Y. Choi, and Y. Han, "Field trial of millimeter-wave-based MHN system for vehicular communications," in *Proc. 12th Eur. Conf. Antennas Propag. (EuCAP)*, London, U.K., Apr. 2018, pp. 1–5.
- [20] *NR; Base Station (BS) Radio Transmission and Reception*, 3GPP, document TS 38.104, 2022.
- [21] A. Ikami, T. Hayashi, T. Nagao, and Y. Amano, "A novel method to estimate propagation for spectrum sharing between 5G mm wave access and wireless backhaul," in *Proc. IEEE Asia-Pacific Microw. Conf. (APMC)*, Dec. 2019, pp. 1068–1070.
- [22] J. Wu and P. Fan, "A survey on high mobility wireless communications: Challenges, opportunities and solutions," *IEEE Access*, vol. 4, pp. 450–476, 2016.
- [23] M. Lerch, P. Svoboda, D. Maierhofer, J. Resch, A. Brantner, V. Raida, and M. Rupp, "Measurement based modelling of in-train repeater deployments," in *Proc. IEEE 89th Veh. Technol. Conf.*, Kuala Lumpur, Malaysia, Apr. 2019, pp. 1–6.
- [24] X. Dong, P. Li, Q. Yu, and Y. Zhu, "A vehicle-ground integration information network scheme based on small base stations," *Electronics*, vol. 11, no. 12, p. 1824, Jun. 2022.
- [25] F. Haider, C.-X. Wang, B. Ai, H. Haas, and E. Hepsaydir, "Spectral energy efficiency trade-off of cellular systems with mobile femtocell deployment," *IEEE Trans. Veh. Technol.*, vol. 65, no. 5, pp. 3389–3400, May 2015.
- [26] X. Zhao, C. Hu, and Z. Li, "Multi-operator radio access network sharing for 5G SA network," in *Proc. Int. Wireless Commun. Mobile Comput. (IWCMC)*, Harbin, China, Jun. 2021, pp. 187–193.
- [27] L. Yan, X. Fang, and Y. Fang, "Stable beamforming with low overhead for C/U-plane decoupled HSR wireless networks," *IEEE Trans. Veh. Technol.*, vol. 67, no. 7, pp. 6075–6086, Jul. 2018.
- [28] *NR; User Equipment (UE) Radio Transmission and Reception; Part 2: Range 2 Standalone*, 3GPP, document TS 38.101-2, 2022.
- [29] Q. Xingyu, "Simulation and measurement of millimeter wave propagation characteristics in complex tunnel environment," masters dissertation, Electron. Commun. Eng. Dept., Nanjing Univ. Posts Telecommun., Nanjing, China, Jun. 2017.
- [30] *NR; Physical Channels and Modulation*, 3GPP, document TS 38.211, 2022.
- [31] J. Minghua, Z. Guoxin, and W. Hui, "Fading characteristics of radio propagation in one-way semicircular subway tunnel at 38 GHz," in *Proc. China-Jpn. Joint Microw. Conf.*, Jaipur, India, Sep. 2008, pp. 529–530.
- [32] D. G. Dudley, "Wireless propagation in circular tunnels," *IEEE Trans. Antennas Propag.*, vol. 53, no. 1, pp. 435–441, Jan. 2005.
- [33] M. Jia, "The propagation characteristics of millimeter wave in subway tunnels," doctoral dissertation, Commun. Commun. Syst. Dept., Shanghai Univ., Shanghai, China, Apr. 2010.
- [34] I. K. Jain, "Millimeter wave beam training: A survey," 2018, *arXiv:1810.00077*.
- [35] X. Zhao, G. Liu, P. Li, Z. Li, C. Hu, and W. Xie, "Multi independent logical cells under 5G radio access network sharing of mobile operators," in *Proc. IEEE Int. Symp. Broadband Multimedia Syst. Broadcast. (BMSB)*, Jun. 2022, pp. 1–5.
- [36] J. Mendoza, I. de-la-Bandera, C. S. Álvarez-Merino, E. J. Khatib, J. Alonso, S. Casalderrey-Díaz, and R. Barco, "5G for construction: Use cases and solutions," *Electronics*, vol. 10, no. 14, p. 1713, Jul. 2021.
- [37] G. Noh, J. Kim, H. Chung, and I. Kim, "Realizing multi-Gbps vehicular communication: Design, implementation, and validation," *IEEE Access*, vol. 7, pp. 19435–19446, 2019.



XIAOYIN ZHAO received the master's degree in communication engineering from the Technical University of Berlin, Germany, in January 2009. She is currently a Senior Engineer with the Mobile Communication and Terminal Technology Research Department, China Telecom Corporation Ltd. Beijing Research Institute, Beijing. She has published many academic articles and patents. Her research interests include mobile networks, wireless communication systems, and network planning.



FEI QI (Member, IEEE) received the Ph.D. degree from the Beijing University of Posts and Telecommunications, China, in 2022. He is currently the Technical Director of China Telecom Corporation Ltd. Beijing Research Institute. He is active in standards development, such as ITU-R WP5D and CCSA. He is responsible for the spectrum simulation projects as the Project Leader. He has published many academic articles and patents. His current research interests include the Internet of Things, vehicular networks, massive-MIMO precoding, artificial intelligence, and channel estimation.



WEILIANG XIE received the Ph.D. degree in information science and technology from Peking University, Beijing, China, in 2003. He is currently a Senior Engineer and the Deputy Director of the Mobile Communication and Terminal Technology Research Department, China Telecom Corporation Ltd. Beijing Research Institute, Beijing. He was the Principle Investigator of the National Science and Technology Major Project of China. His current research interests include mobile networks and wireless communication systems.